

A New Grid-Based Monte Carlo Code for Raman Scattered He II

[EvS Meeting] May 15, 2019 @ Sejong University

Bo-Eun Choi (Sejong Univ.)

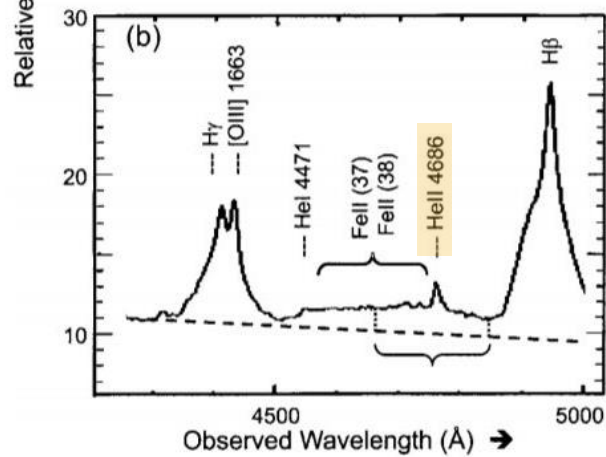
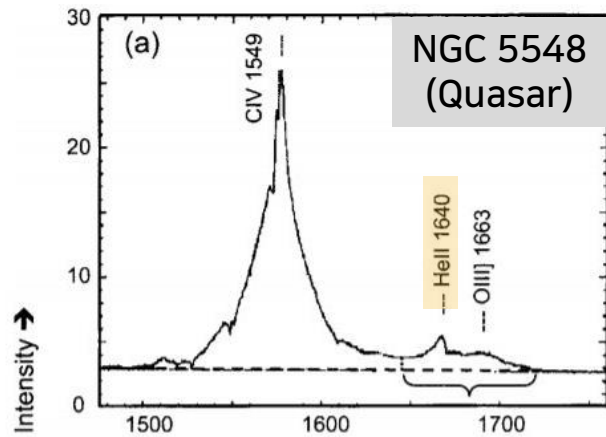
In Collaboration with Seok-Jun Chang & Hee-Won Lee

Contents

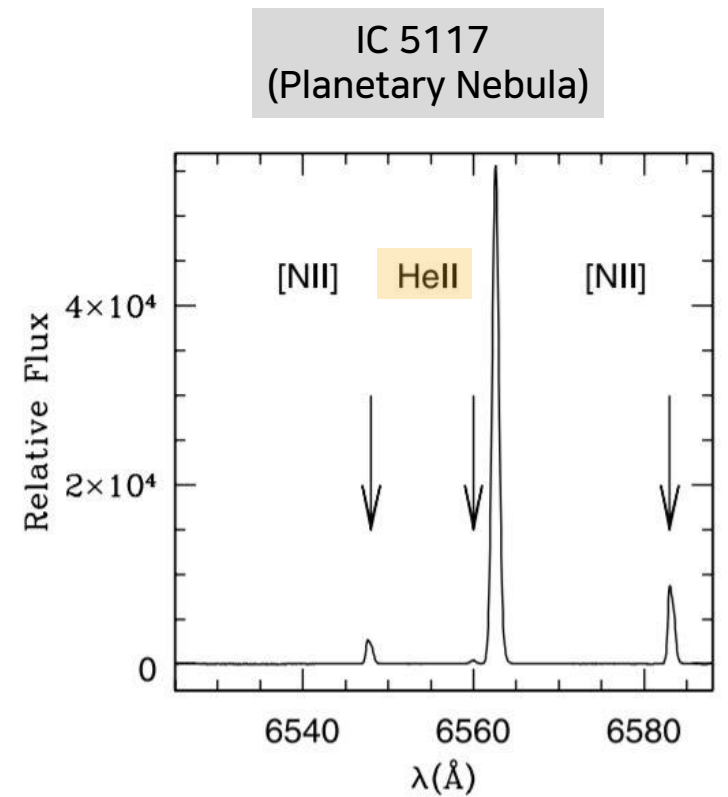
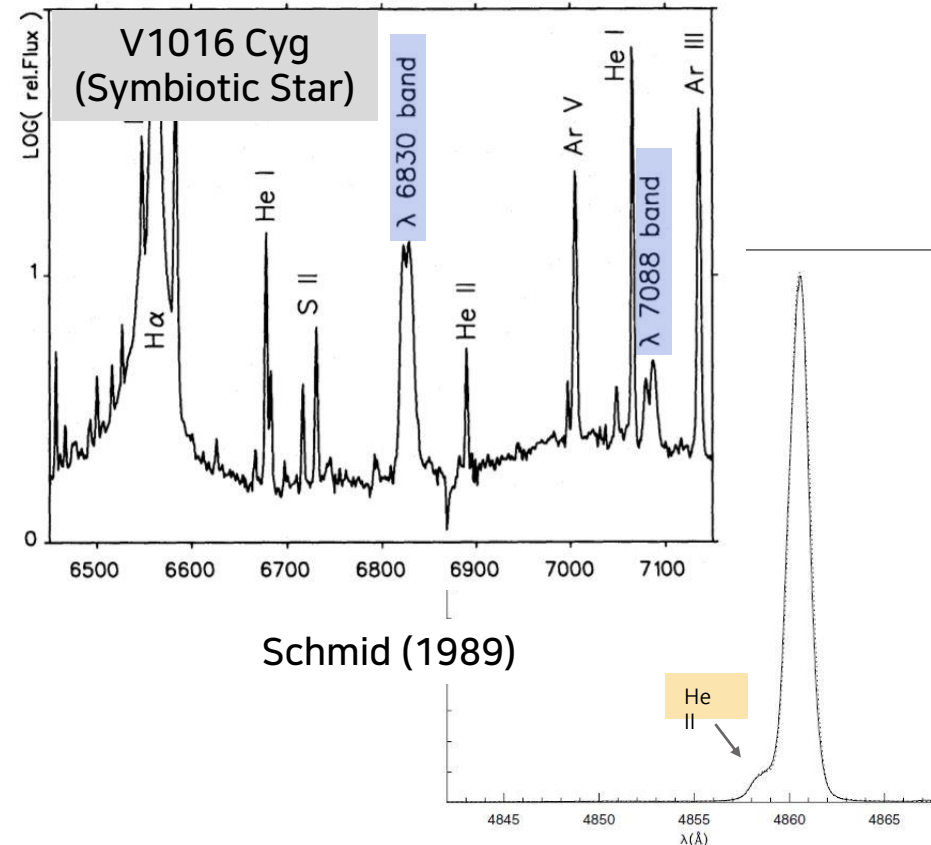
- Introduction
 - Raman Scattered He II
 - Raman He II Features in Symbiotic Stars and Planetary Nebulae
- Grid-Based Radiative Transfer Simulations
- Results

He II Emission

- At high temperature, **He II**, C IV, O VI, O VII ... emission

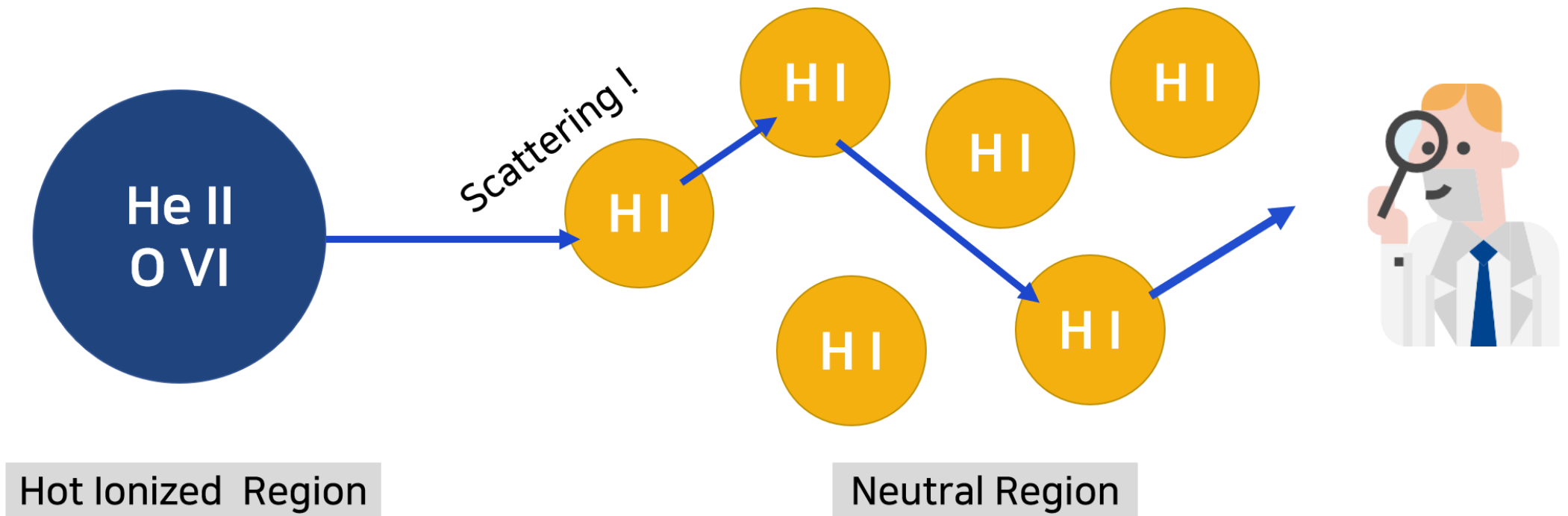


Bottorff et al. (2002)



Lee et al. (2006)

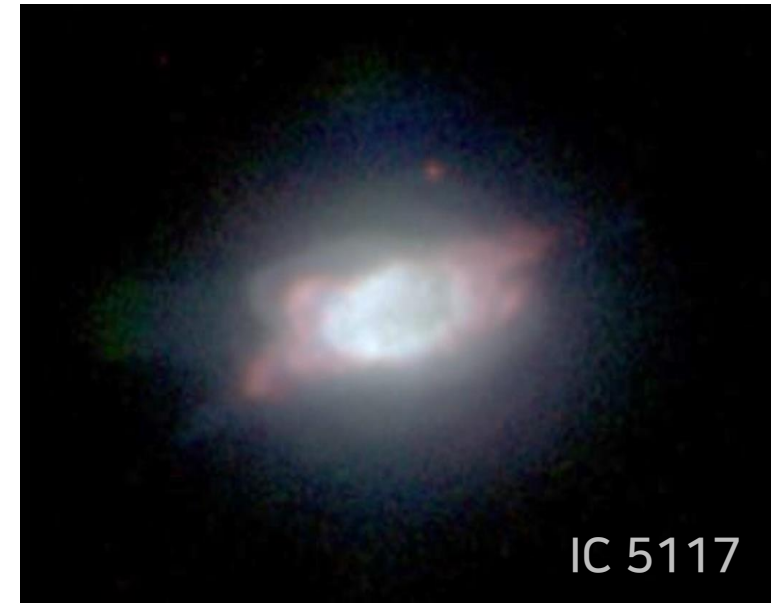
He II Emission



Symbiotic Stars & Planetary Nebulae

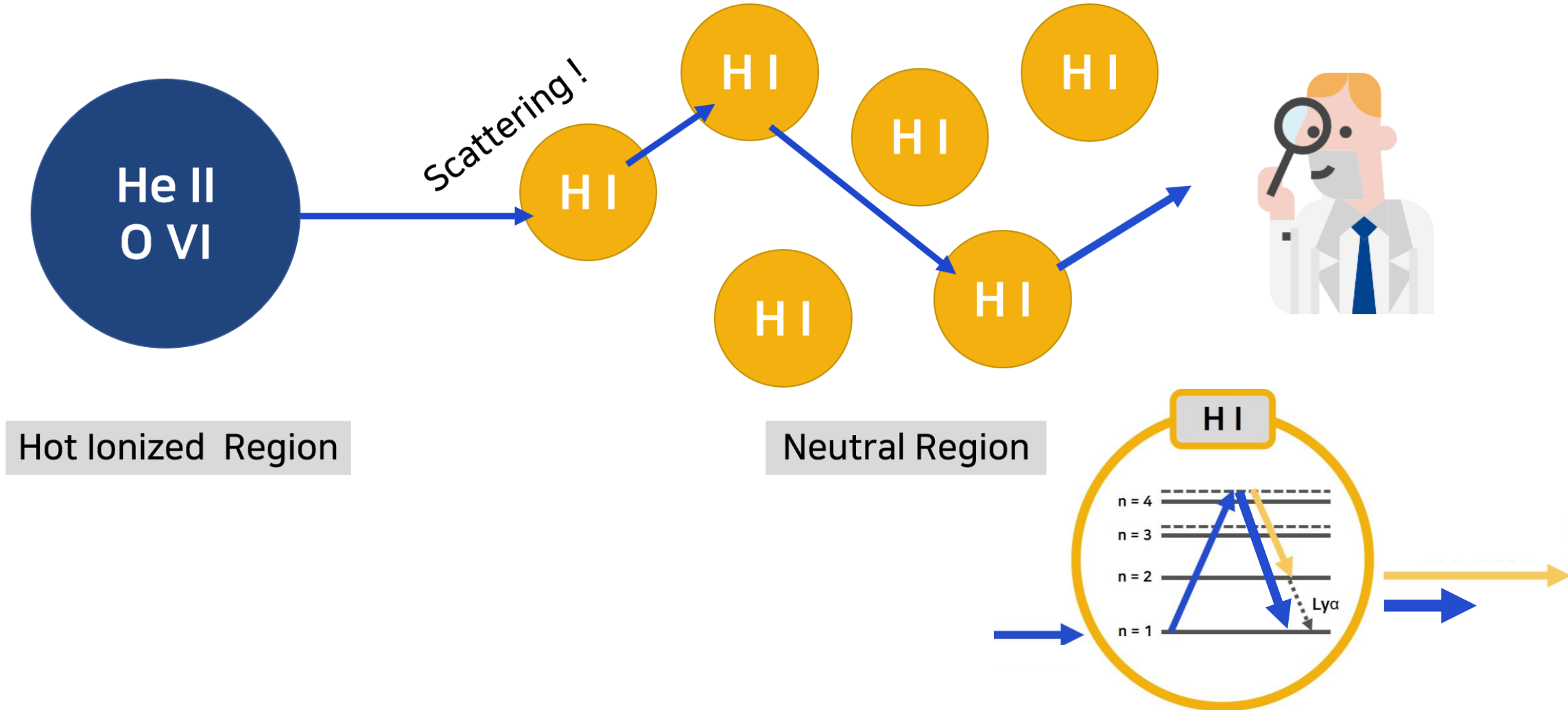


- Wide binary systems
hot white dwarf + mass-losing giant



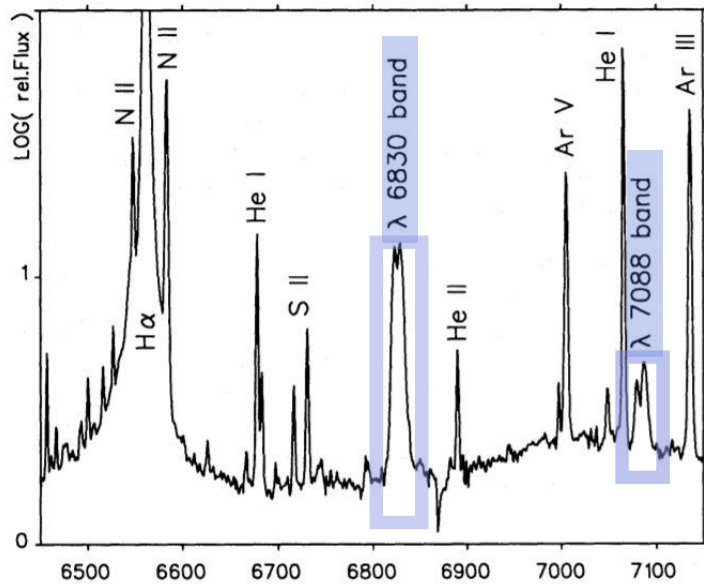
- Young planetary nebulae
- The heavy mass-loss at the giant stage

Symbiotic Stars & Planetary Nebulae

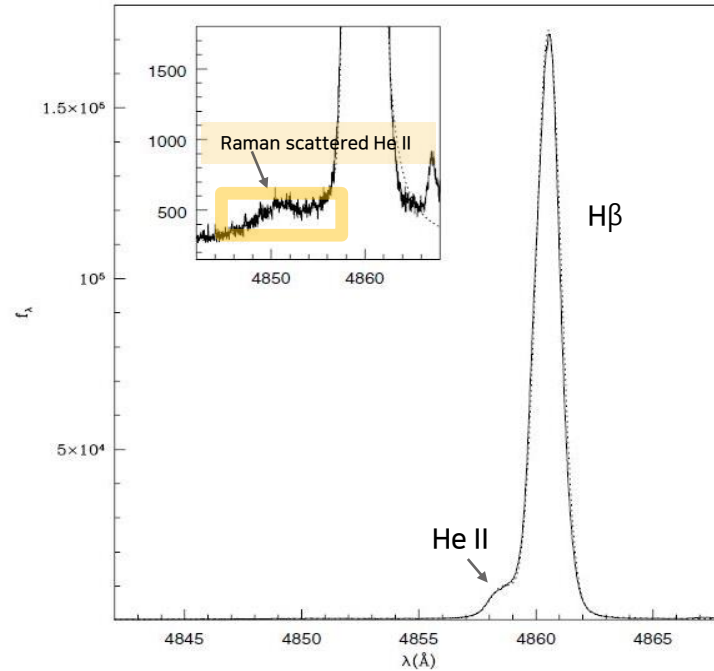


Symbiotic Stars & Planetary Nebulae

V1016 Cyg
(Symbiotic Star)

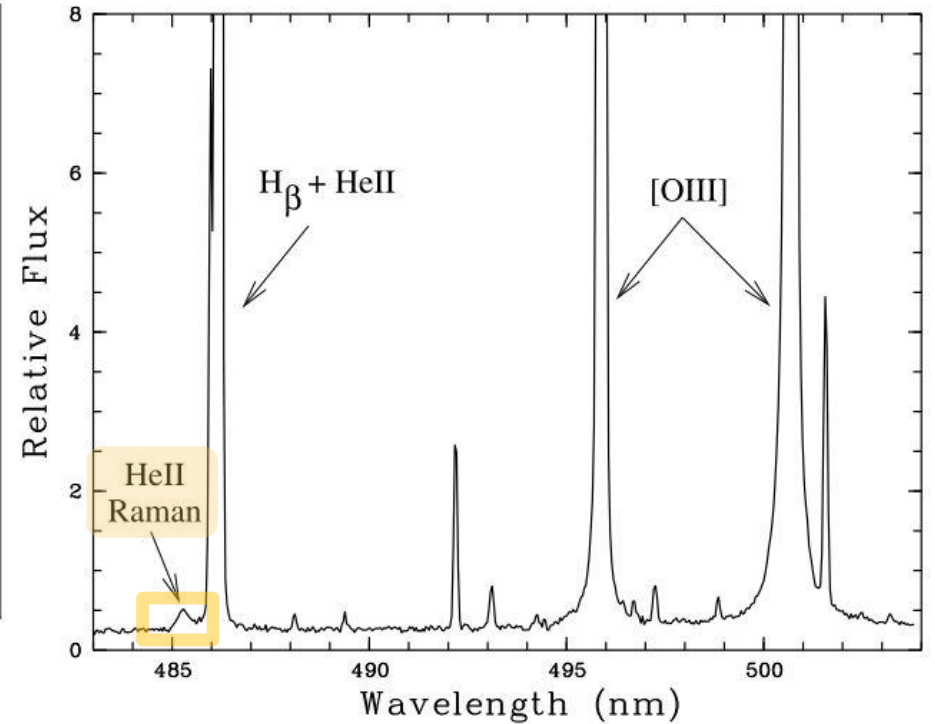


Schmid (1989)



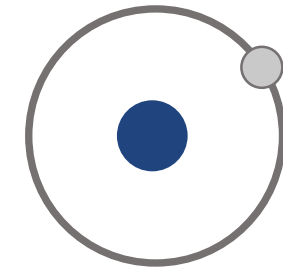
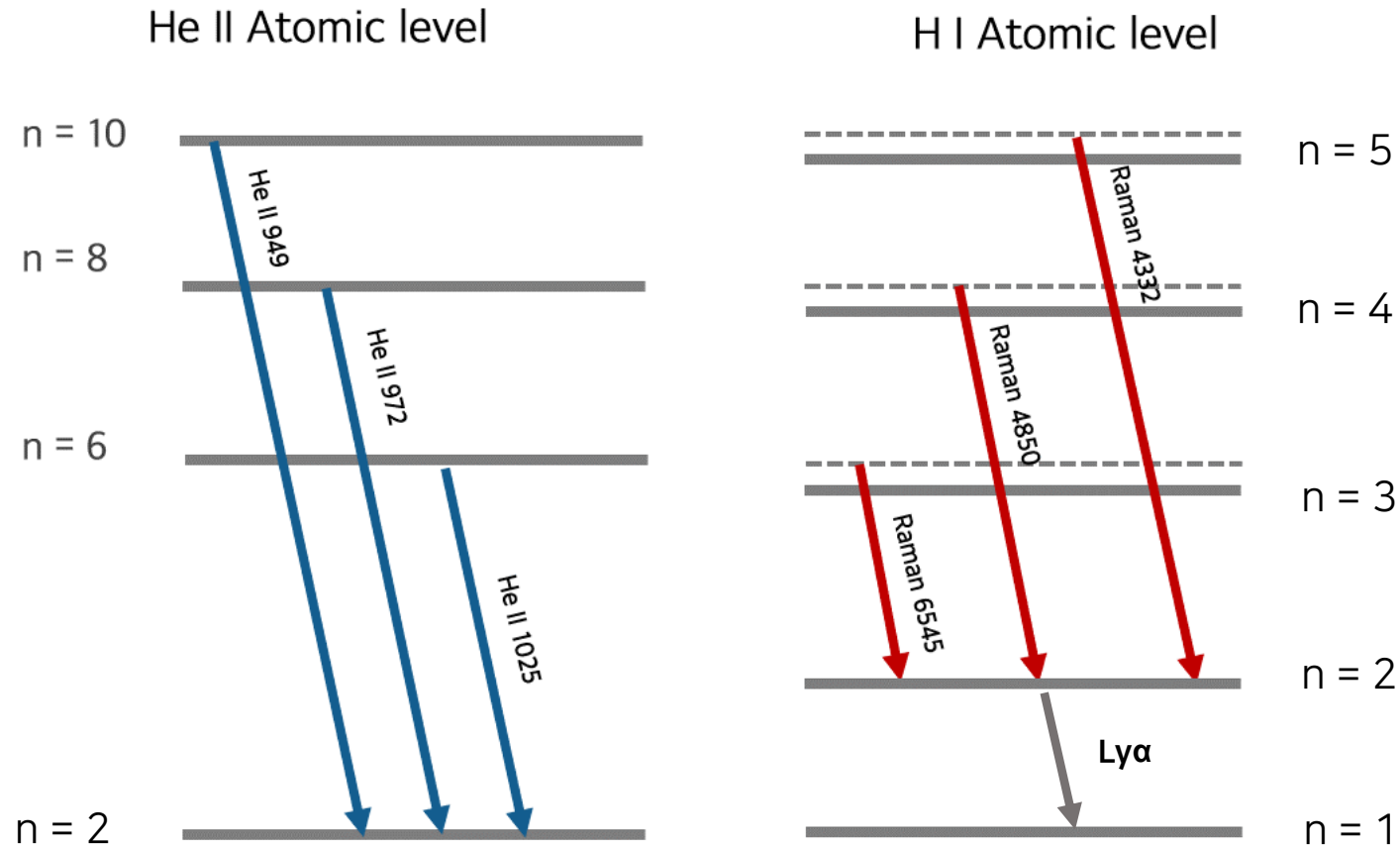
Jung & Lee (2004)

NGC 7027
(Planetary Nebula)



Pequignot et al. (1997)

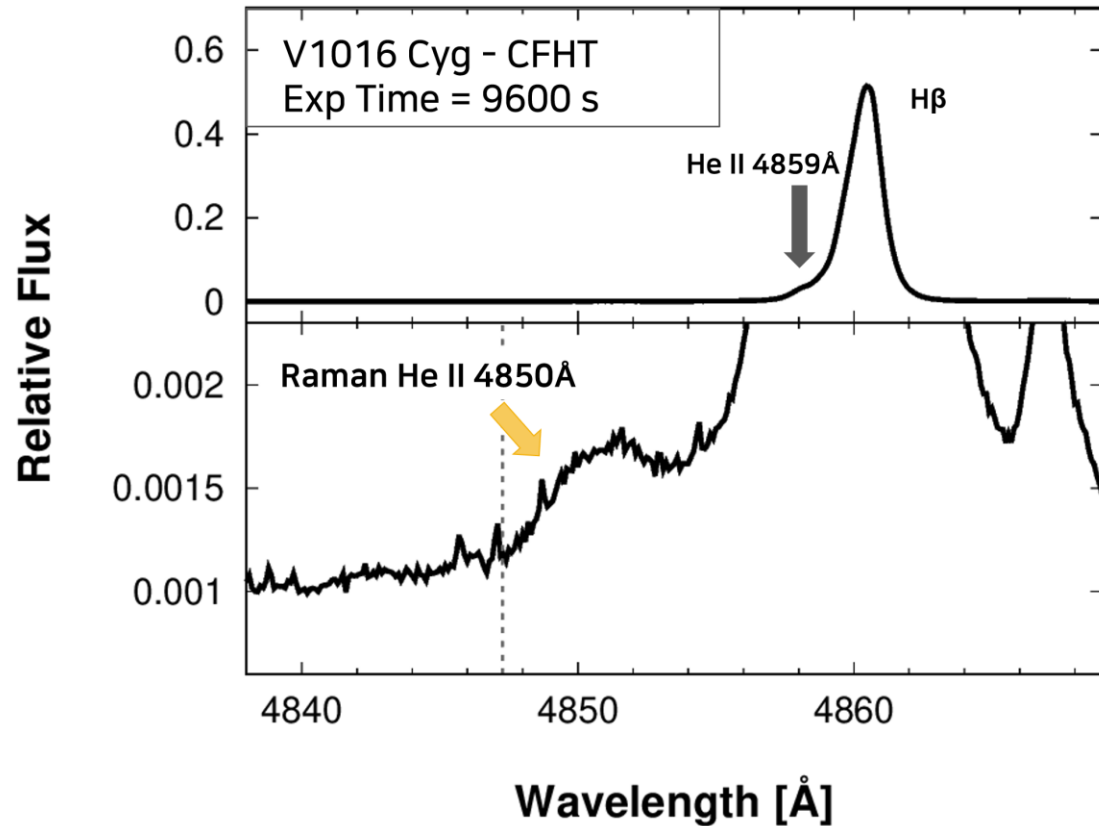
Raman Scattered He II



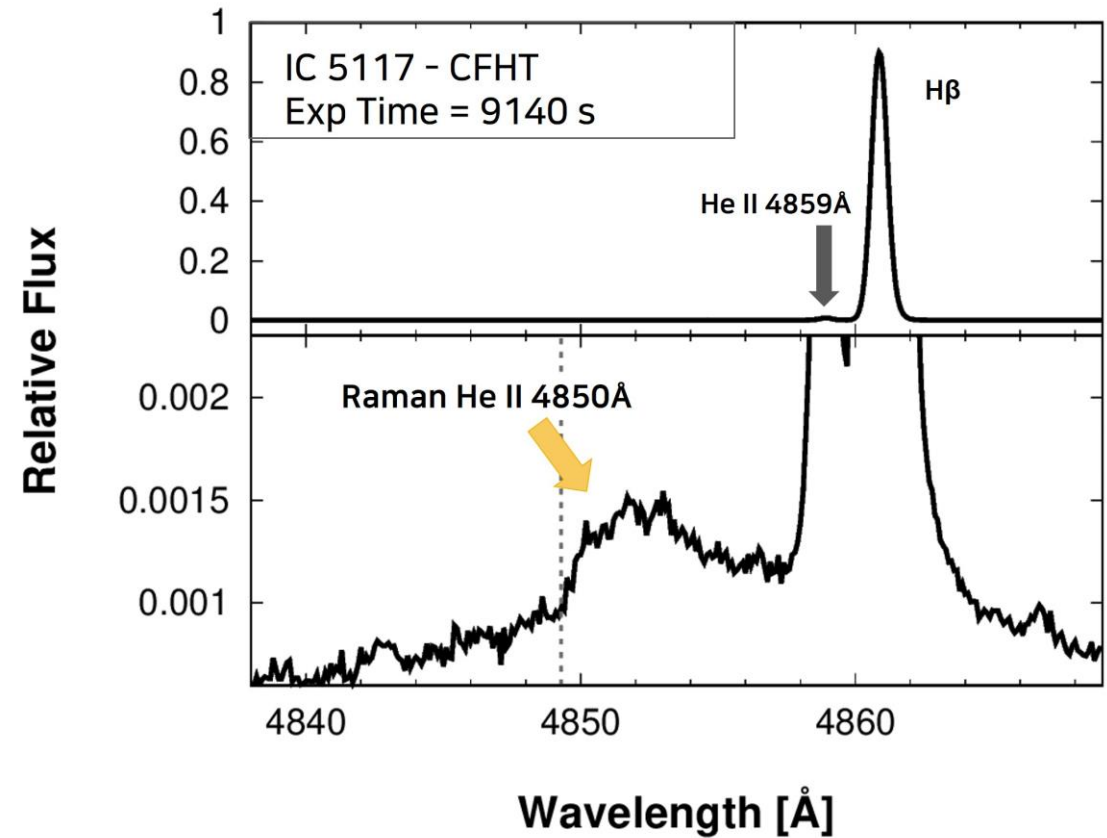
Hydrogen-like ion

- ① He II 1025 \rightarrow 6545 Å
blueward of H α
- ② He II 972 \rightarrow 4850 Å
blueward of H β
- ③ He II 949 \rightarrow 4332 Å
blueward of H γ

Raman He II Features

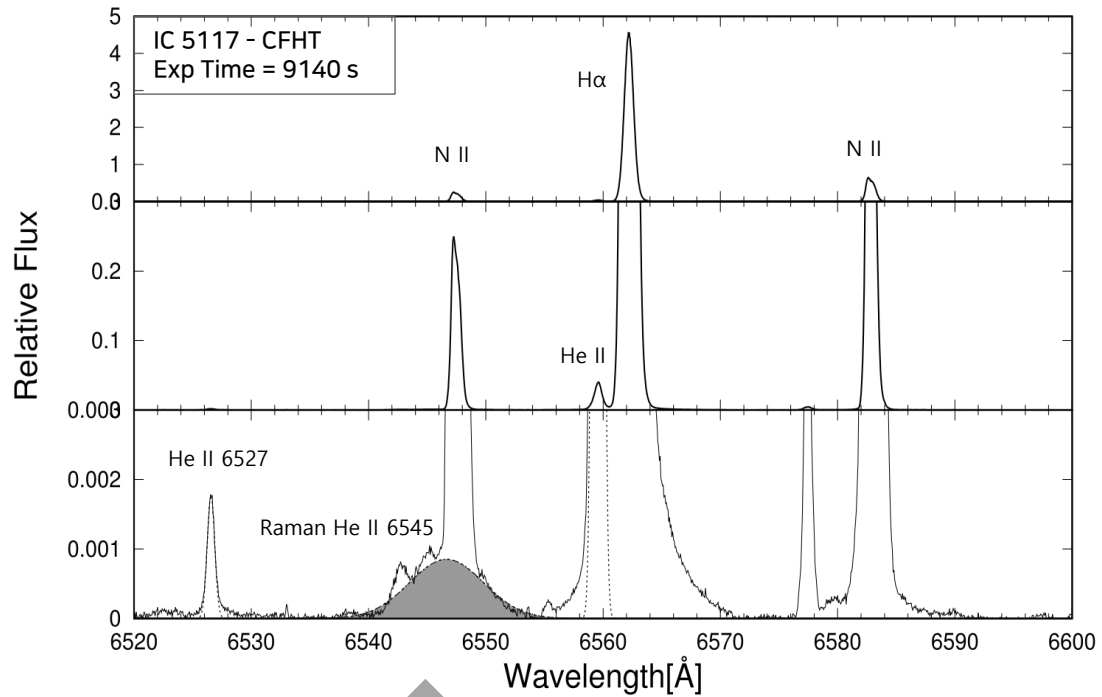


$v_{\text{shift}} = 50 \text{ km/s}$

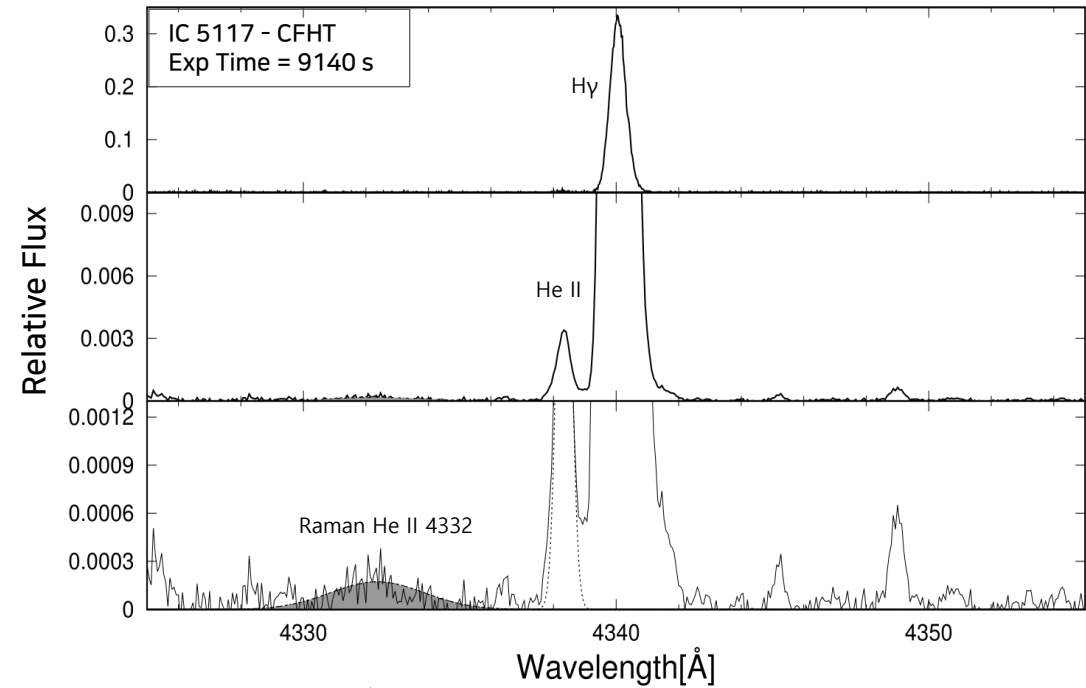


$v_{\text{shift}} = 30 \text{ km/s}$

Raman He II Features

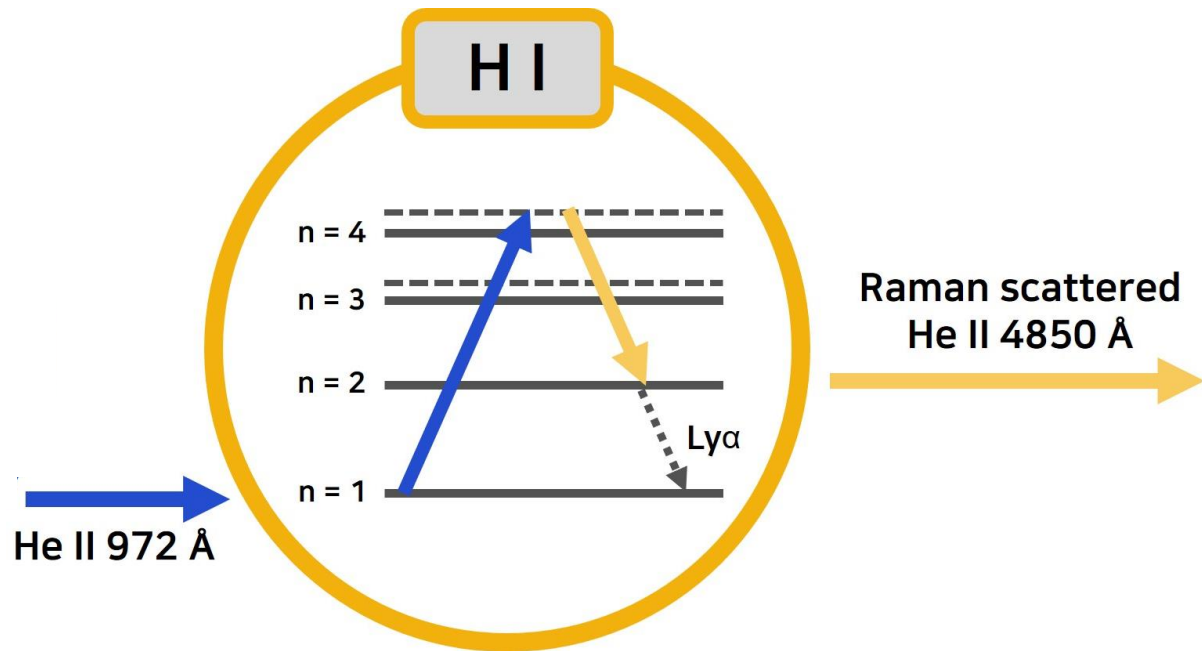


↑
strong N II line



↑
too weak feature
compared with noise

Raman Scattered He II



- $E_f = E_i - E_{Ly\alpha}$

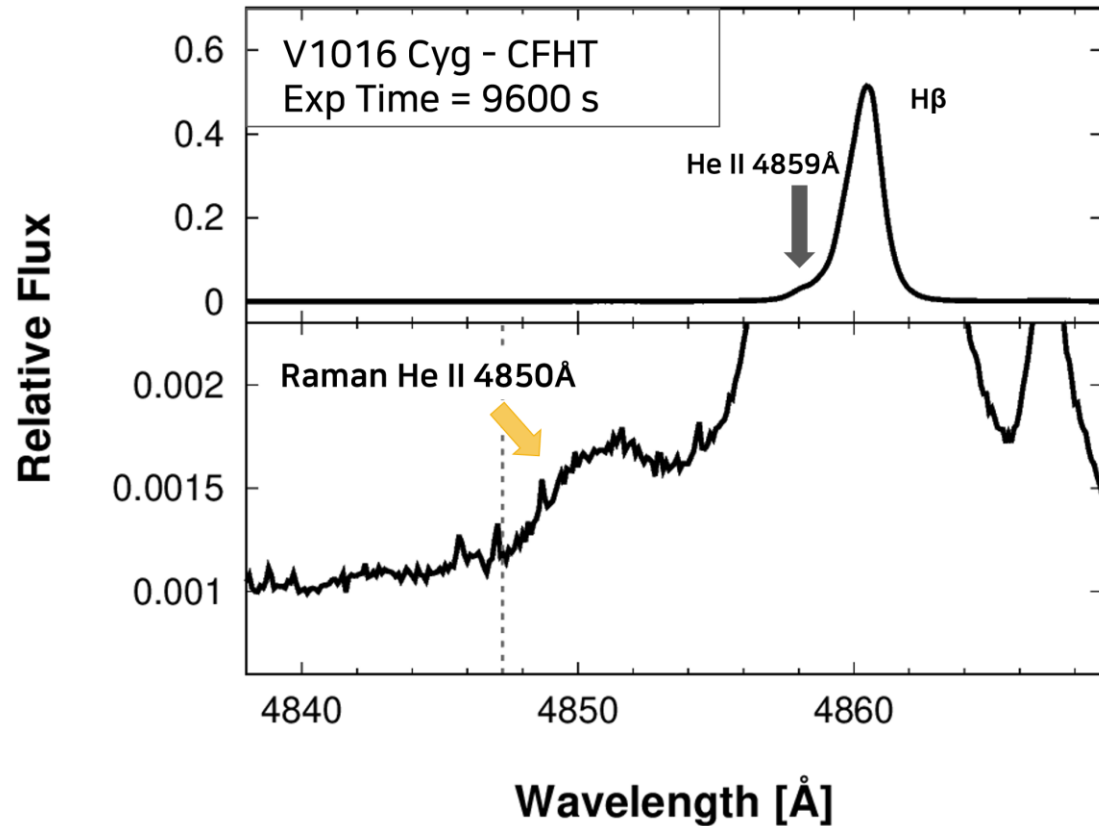
- $\frac{1}{\lambda_f} = \frac{1}{\lambda_i} - \frac{1}{Ly\alpha} \Rightarrow \frac{\Delta\lambda_f}{\lambda_f} = \left(\frac{\lambda_f}{\lambda_i}\right) \frac{\Delta\lambda_i}{\lambda_i}$

In the case of Raman He II 4850 Å,

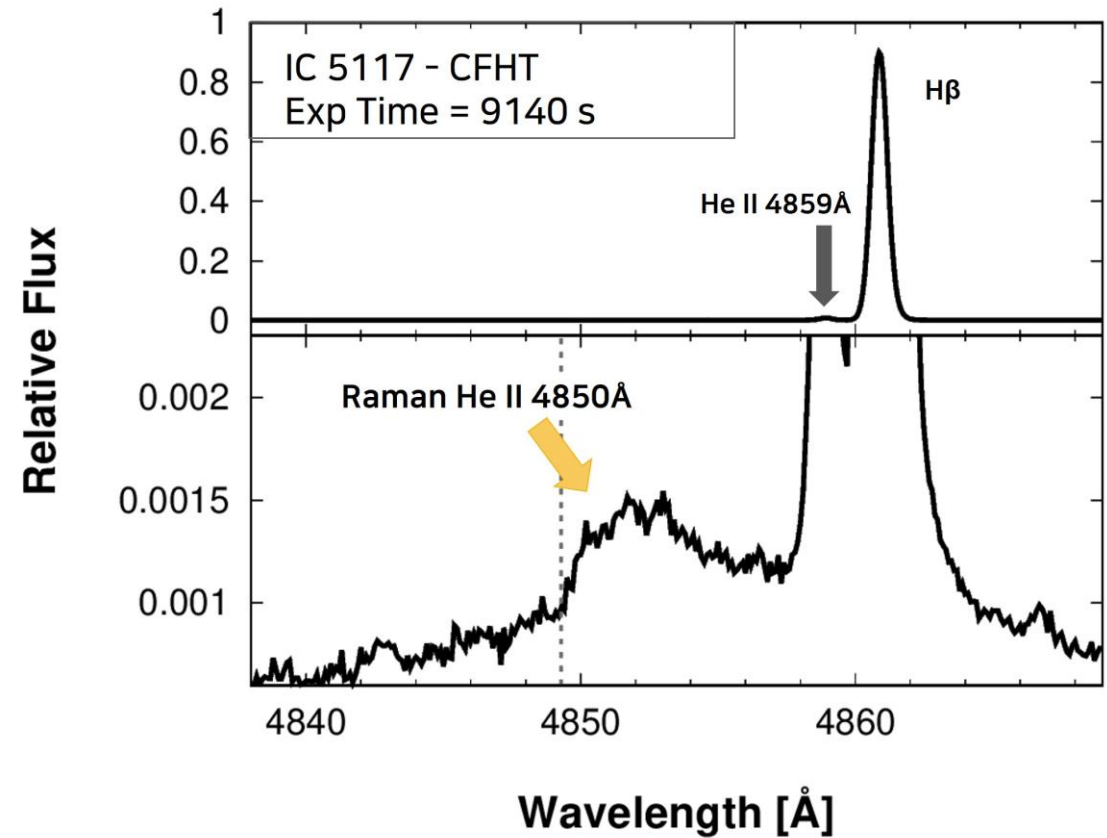
$$\left(\frac{\lambda_f}{\lambda_i}\right) = \left(\frac{4850}{972}\right) \approx 5$$

Raman scattered He II lines are a few times broader than He II emission lines !

Raman He II Features

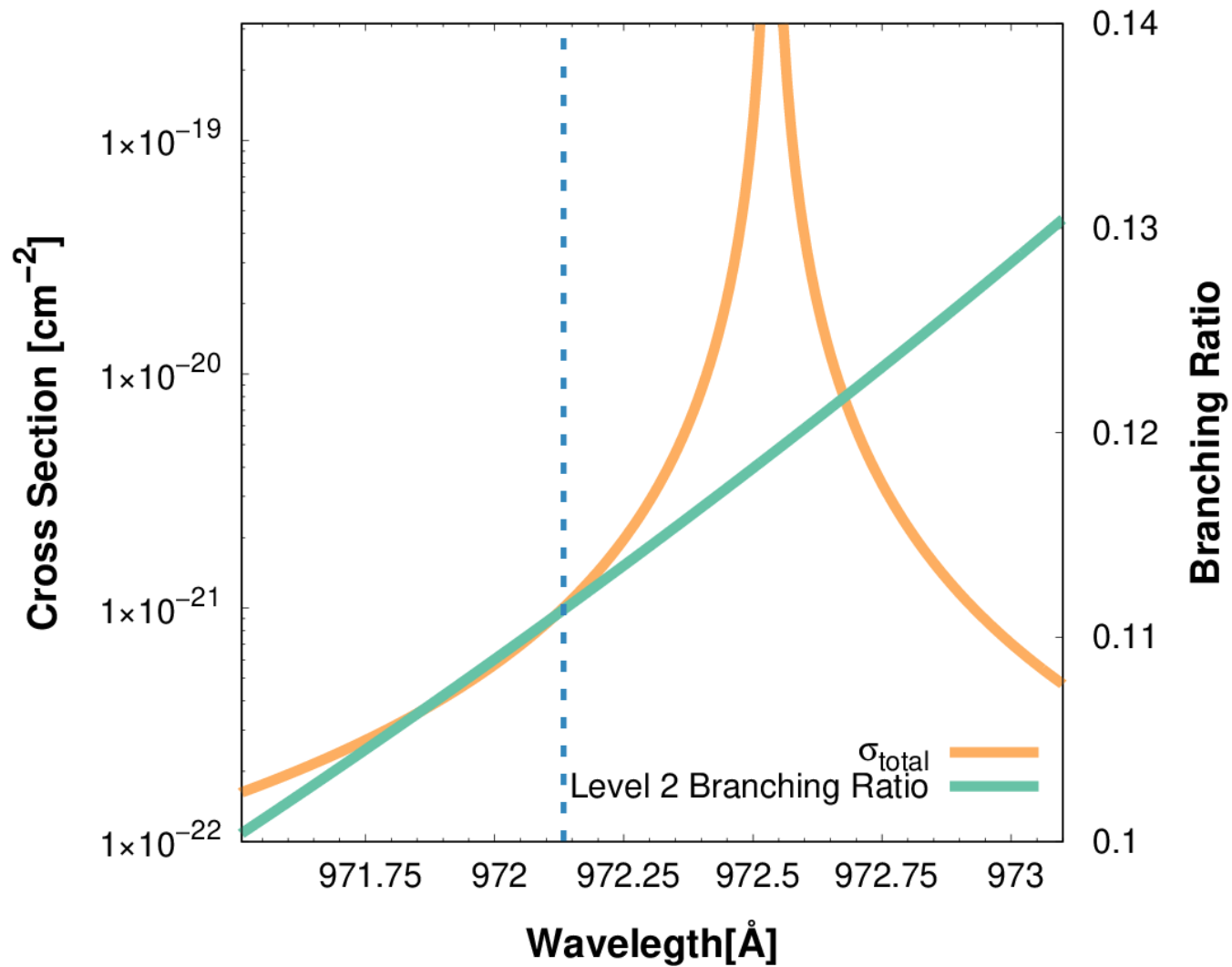


$v_{\text{shift}} = 50 \text{ km/s}$



$v_{\text{shift}} = 30 \text{ km/s}$

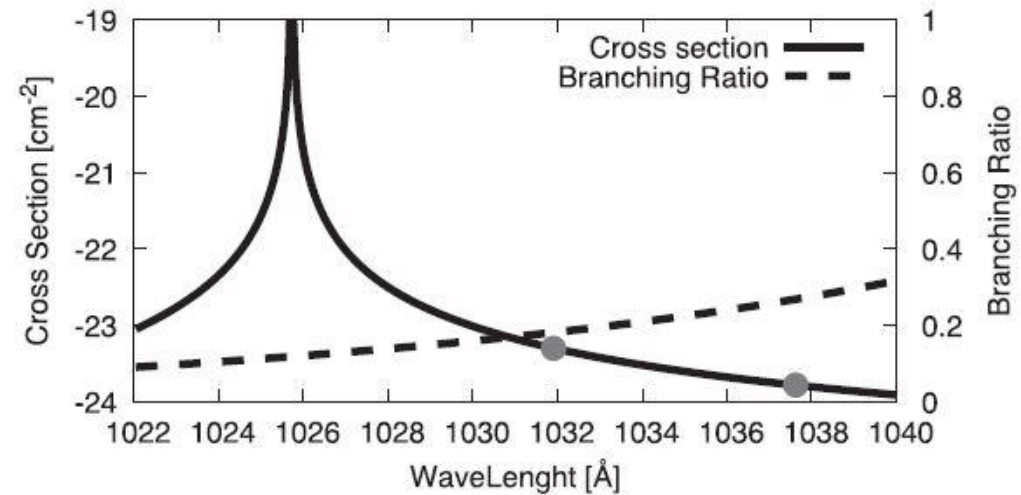
Raman Scattered He II



Raman scattered He II 4850 Å

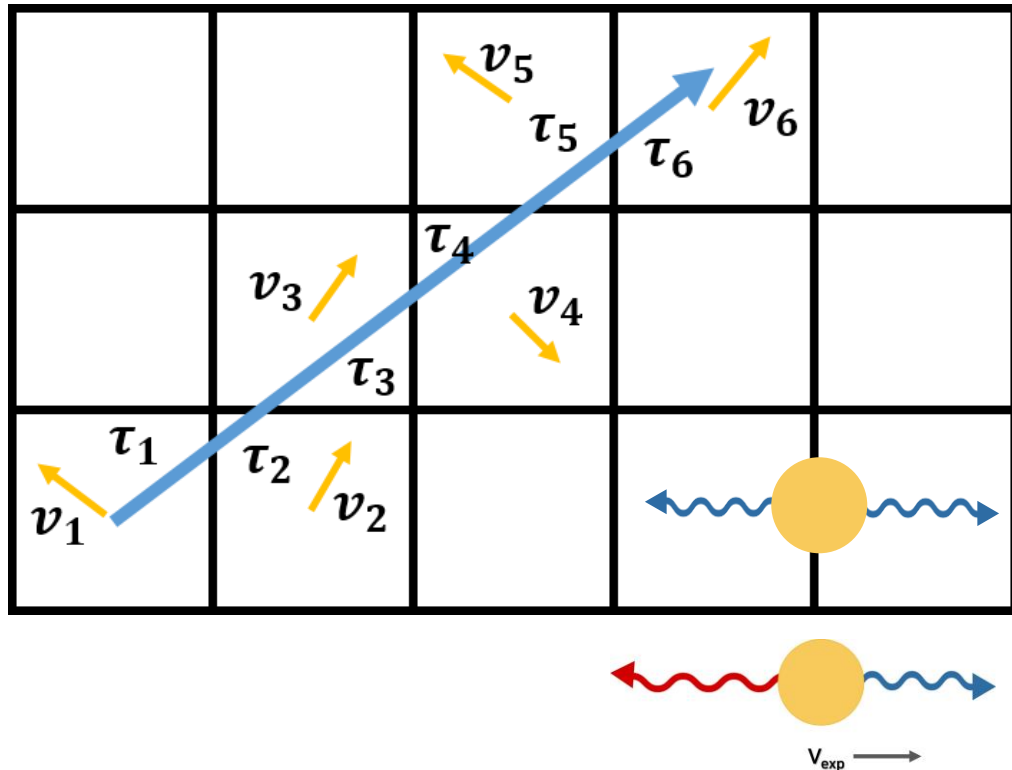
- Branching ratio ≈ 0.11
- $\sigma_{972} \approx 10^{-21} \text{ cm}^2$

For Raman scattering, Thick neutral region with column density $N_{\text{HI}} \approx 10^{21} \text{ cm}^{-2}$ is required



Lee et al. (2016)

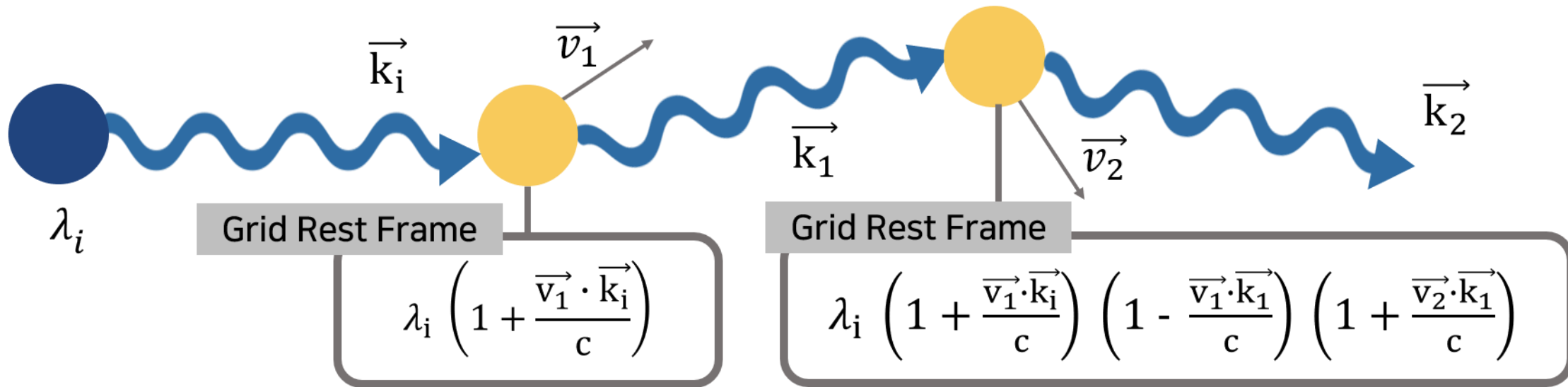
Grid-Based Radiative Transfer



- In each grid, the physical conditions are taken to be uniform.
- A velocity vector and density are assigned to each grid.
- The optical depth τ_i for grid 'i' is computed by multiplying the cross section, density and the path length.
- By adding τ_i through the photon path, we determine the next scattering site.

$$\tau = \tau_1 + \tau_2 + \tau_3 + \tau_4 + \tau_5 + \tau_6$$

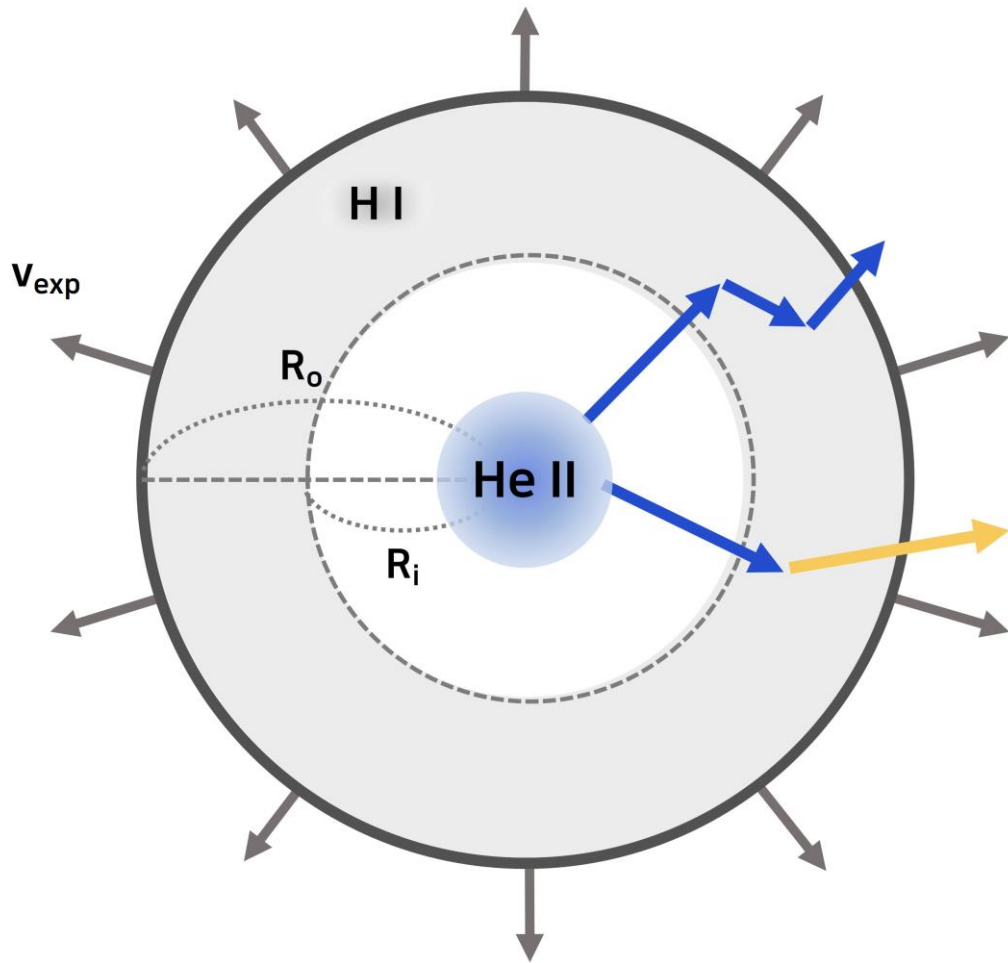
Grid-Based Radiative Transfer



$$\lambda_i \left(1 + \frac{\vec{v}_1 \cdot \vec{k}_i}{c} \right) \left(1 - \frac{\vec{v}_1 \cdot \vec{k}_1}{c} \right)$$

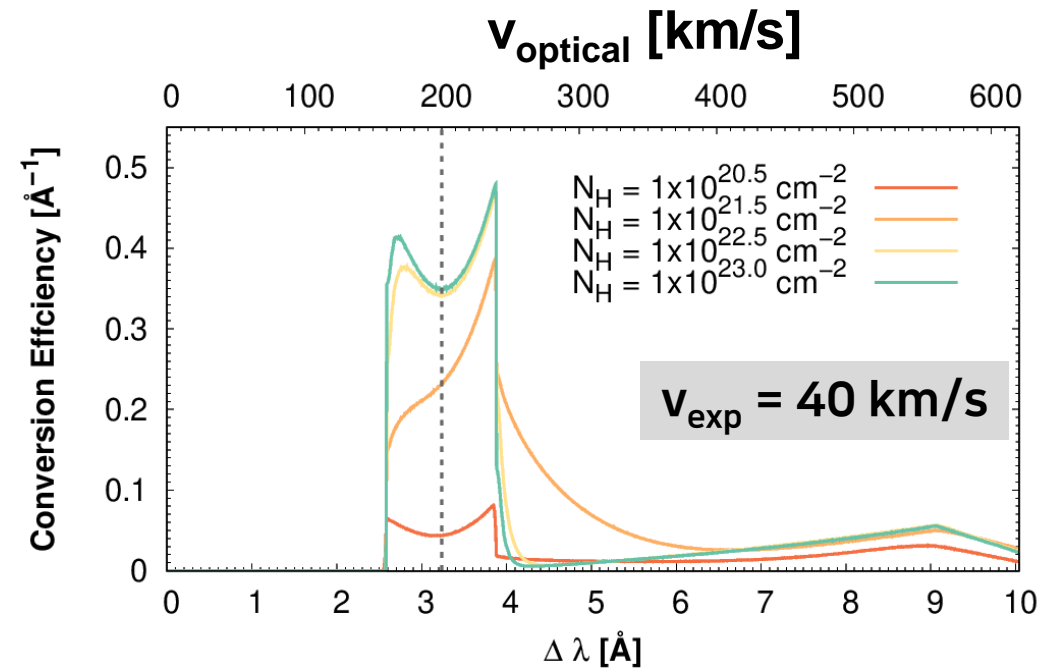
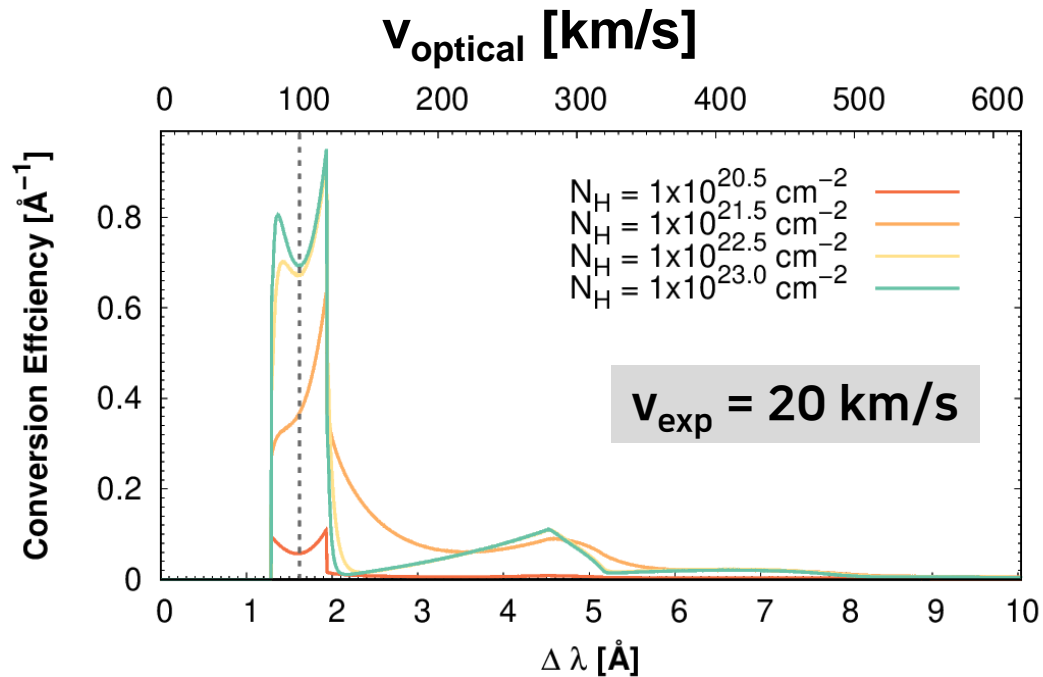
$$\lambda_i \left(1 + \frac{\vec{v}_1 \cdot \vec{k}_i}{c} \right) \left(1 - \frac{\vec{v}_1 \cdot \vec{k}_1}{c} \right) \left(1 + \frac{\vec{v}_2 \cdot \vec{k}_1}{c} \right) \left(1 - \frac{\vec{v}_2 \cdot \vec{k}_2}{c} \right)$$

Geometry of Radiative Transfer



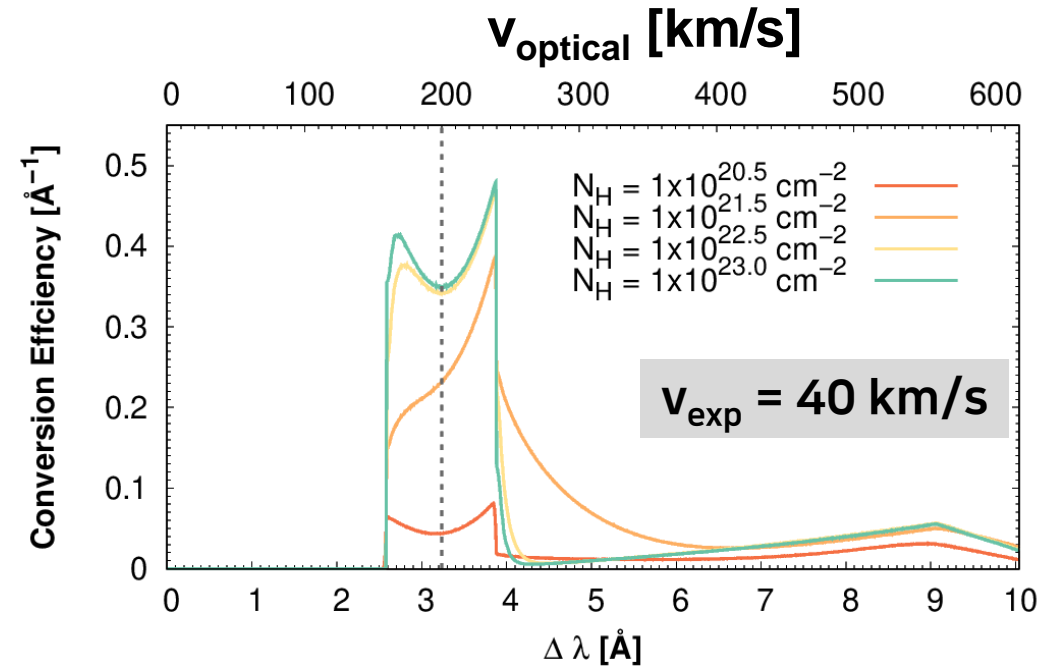
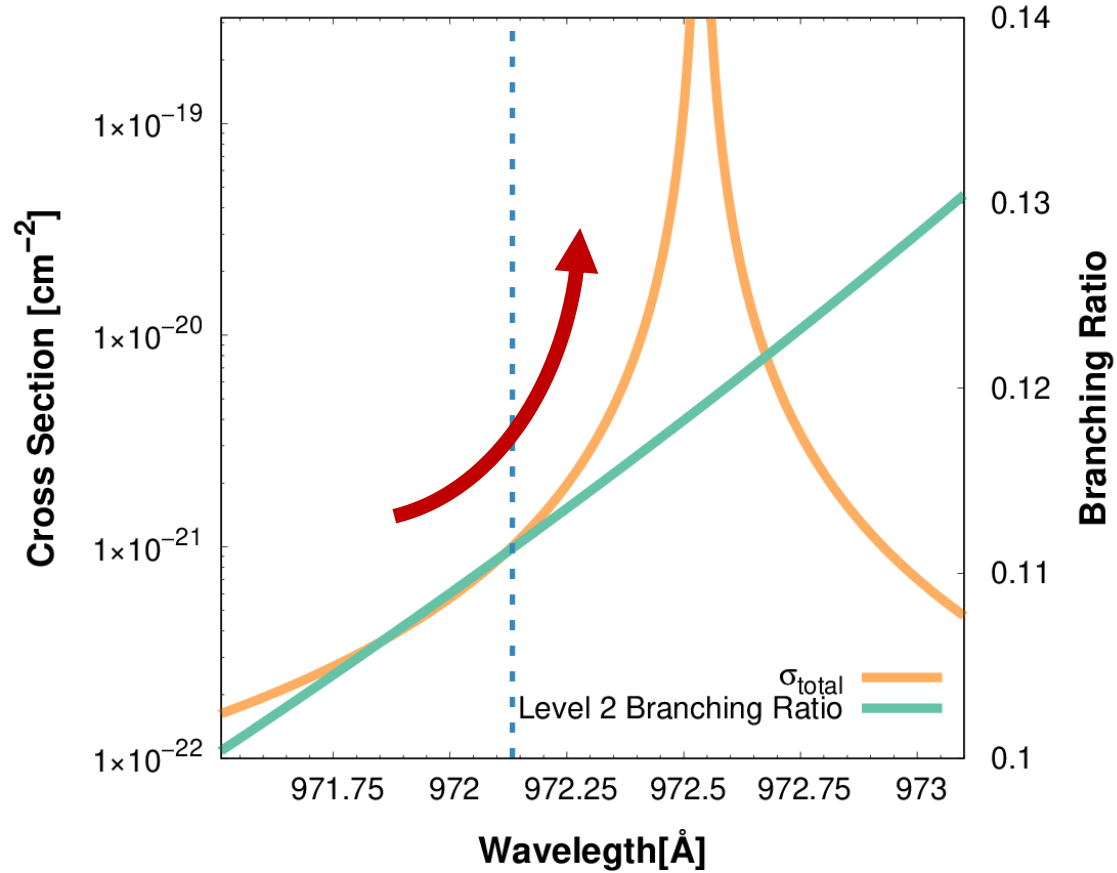
- Assume a **monochromatic / Gaussian He II emission source** is surrounded by a **spherical shell-like H I region**.
- He II UV photons can escape the scattering region by **Rayleigh and Raman scattering**.
- The H I region is moving away from the He II source with **constant velocity v_{exp}** .
- Parameters
 - N_{HI} (column density)
 - v_{exp} (expansion velocity of the H I region)

Result ① : Monochromatic Source

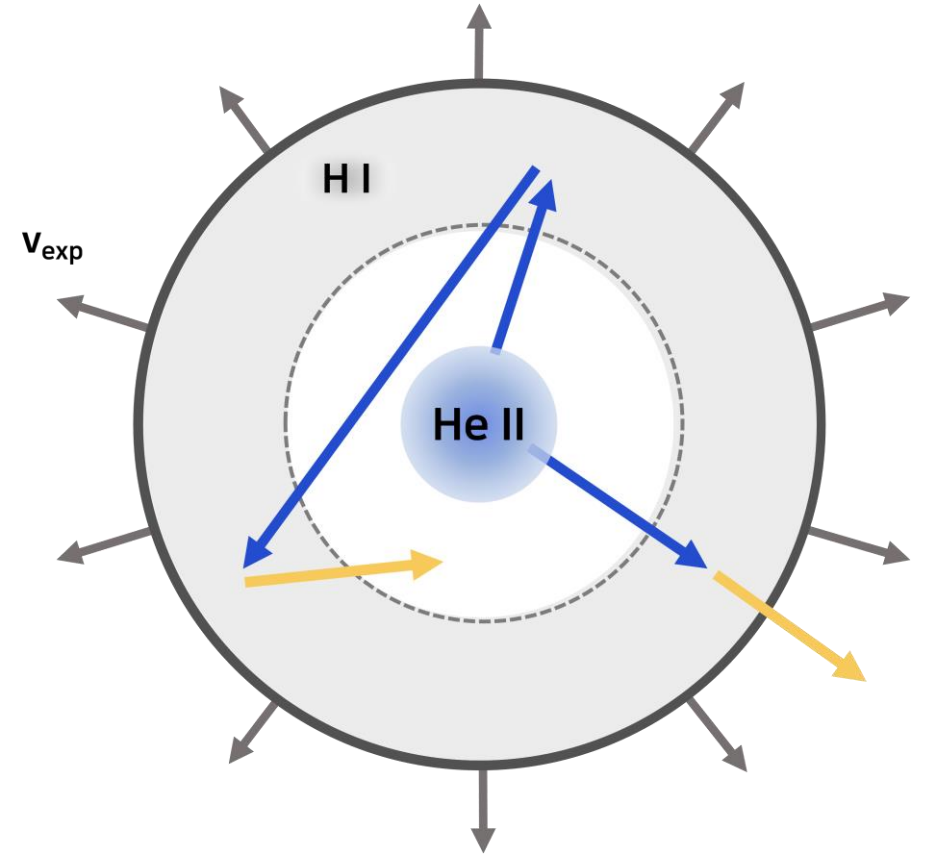
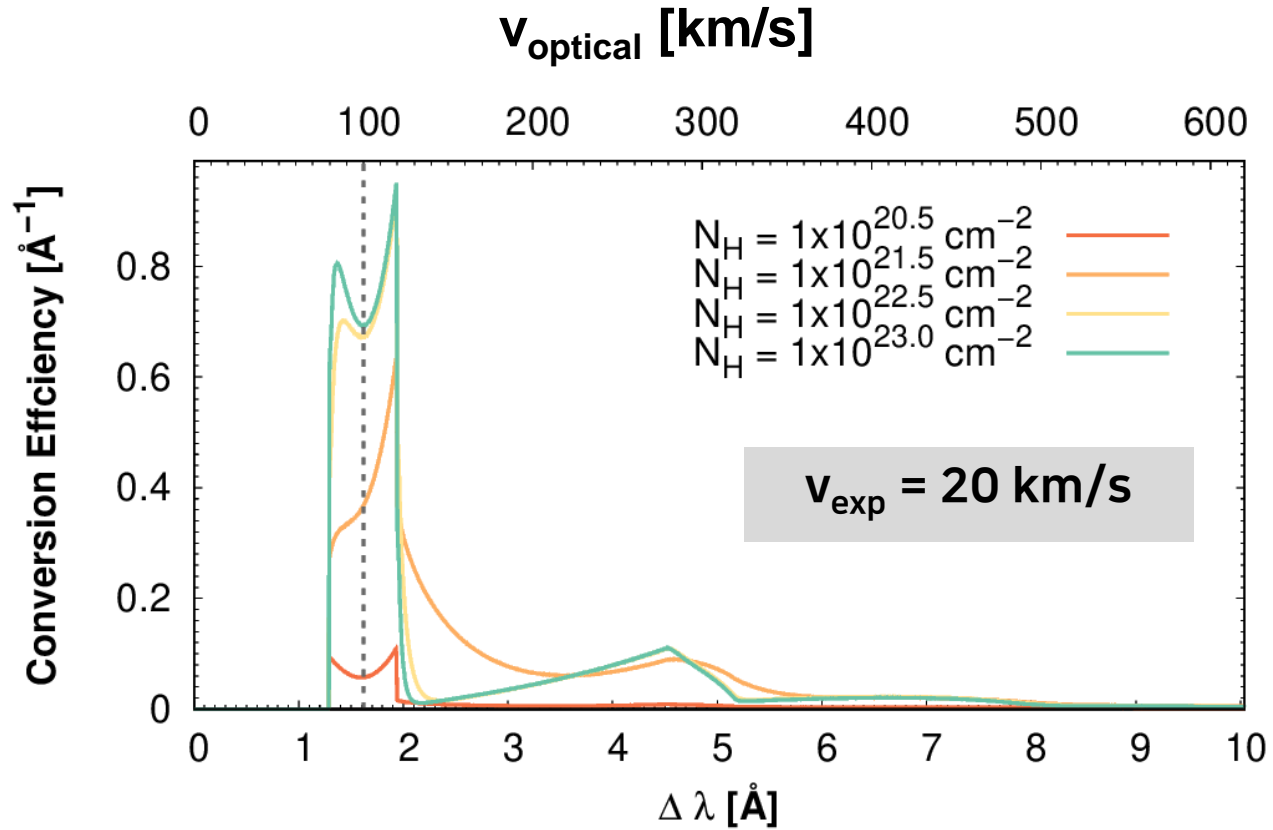


- ① Double peak structure varying with column densities
- ② Appearance of a secondary peak – reentry effect
- ③ The width of primary peak $\approx 2 v_{\text{exp}}$

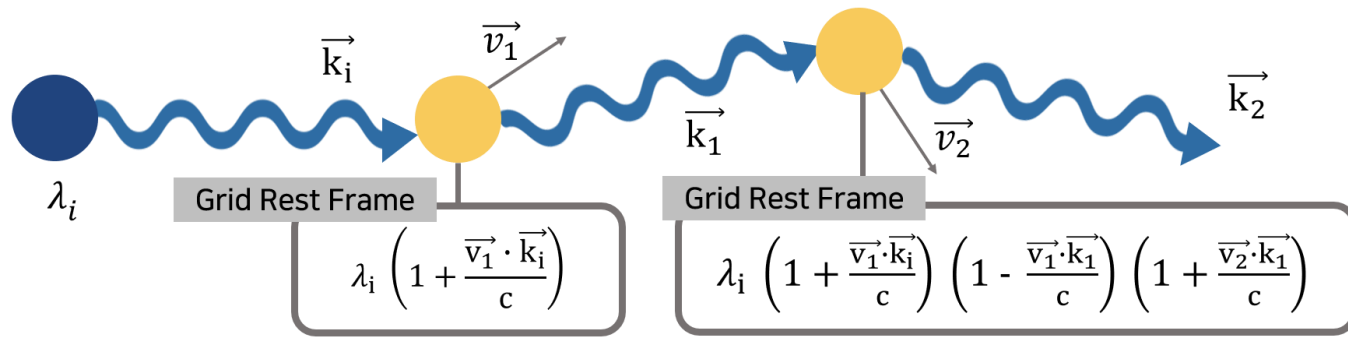
Result ① : Monochromatic Source



Result ① : Monochromatic Source

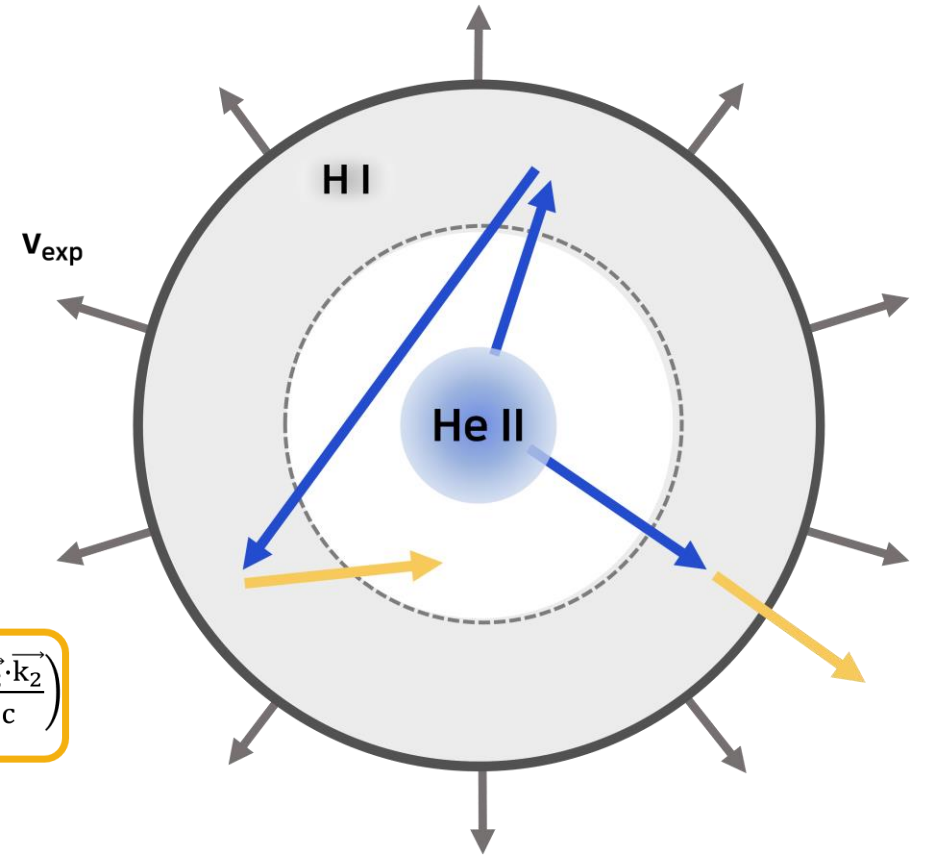


Result ① : Monochromatic Source

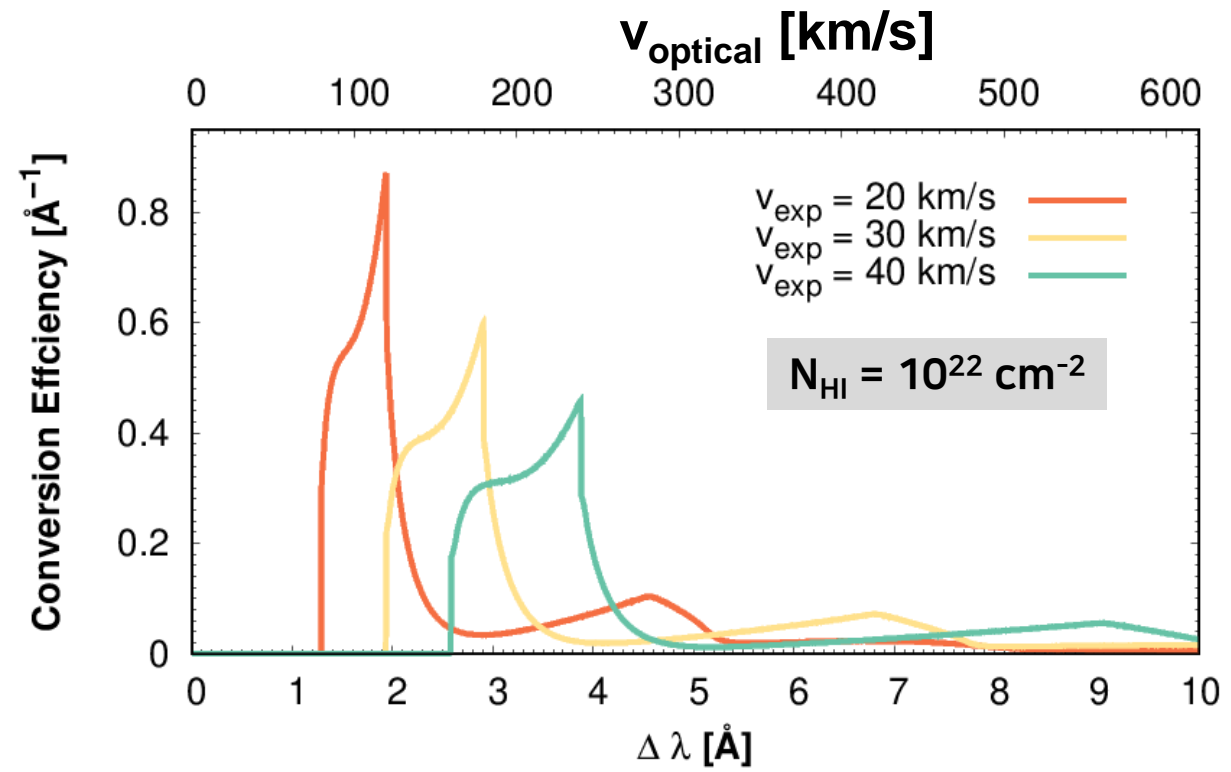
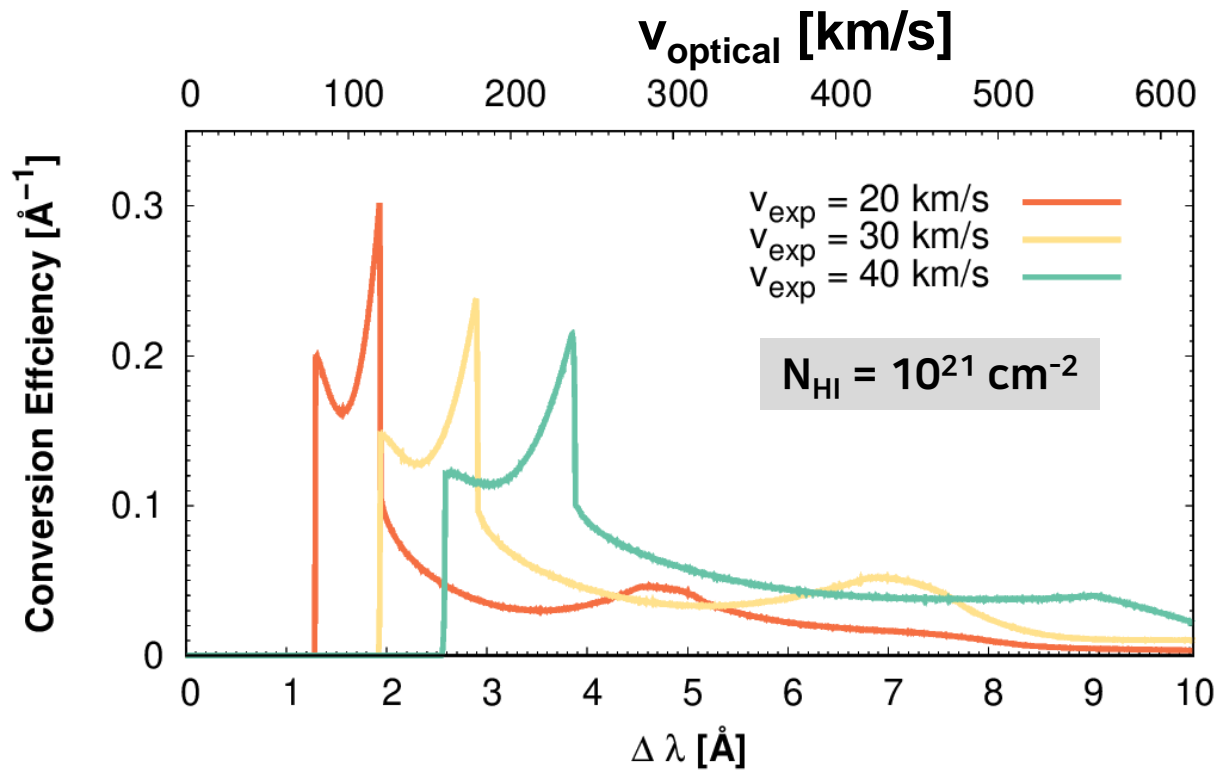


$$\lambda_i \left(1 + \frac{\vec{v}_1 \cdot \vec{k}_i}{c} \right) \left(1 - \frac{\vec{v}_1 \cdot \vec{k}_1}{c} \right)$$

$$\lambda_i \left(1 + \frac{\vec{v}_1 \cdot \vec{k}_i}{c} \right) \left(1 - \frac{\vec{v}_1 \cdot \vec{k}_1}{c} \right) \left(1 + \frac{\vec{v}_2 \cdot \vec{k}_1}{c} \right) \left(1 - \frac{\vec{v}_2 \cdot \vec{k}_2}{c} \right)$$

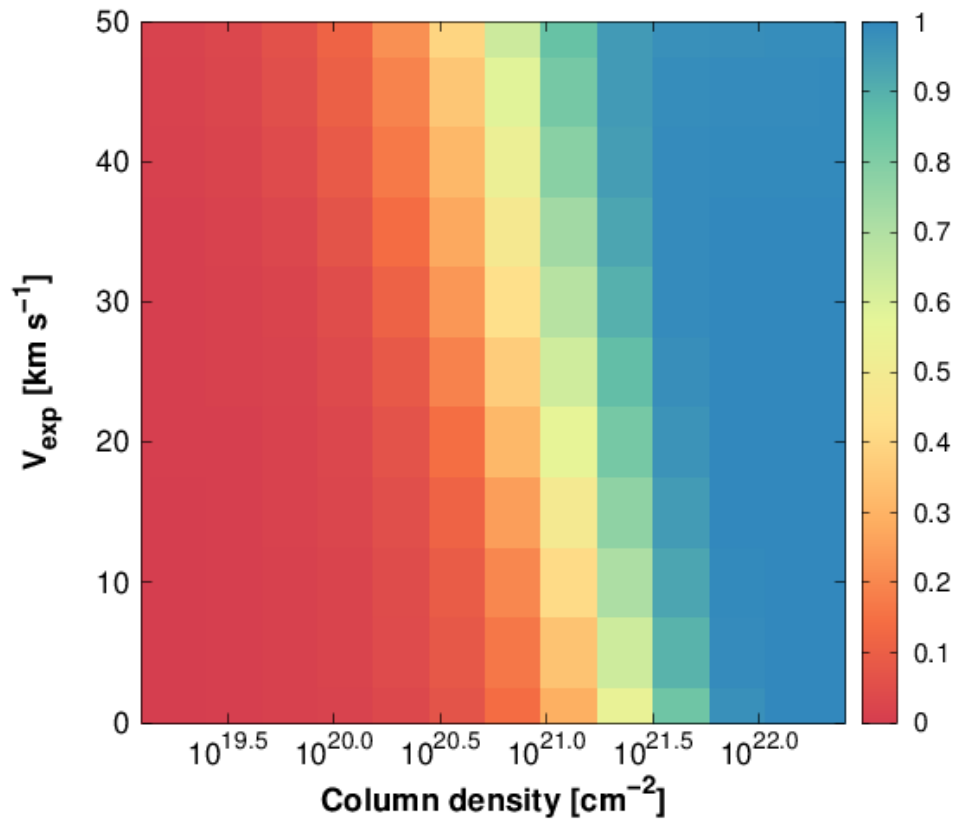


Result ① : Monochromatic Source

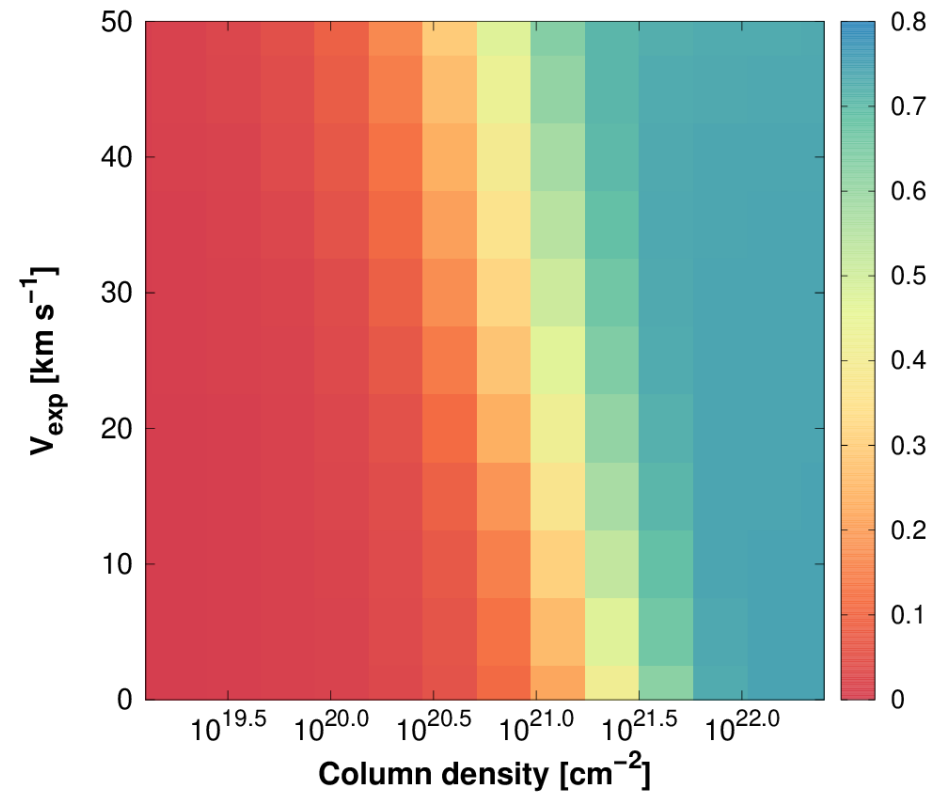


Result ① : Monochromatic Source

Total Raman conversion efficiency

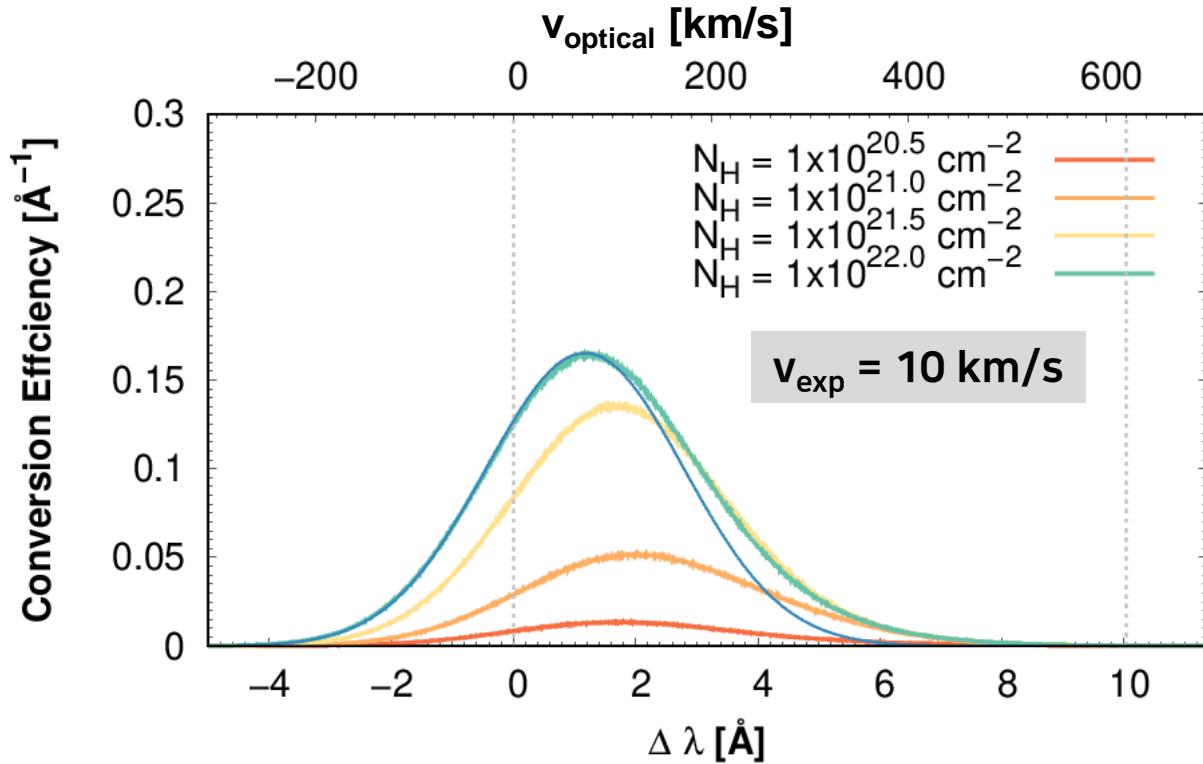


4850 Å conversion efficiency

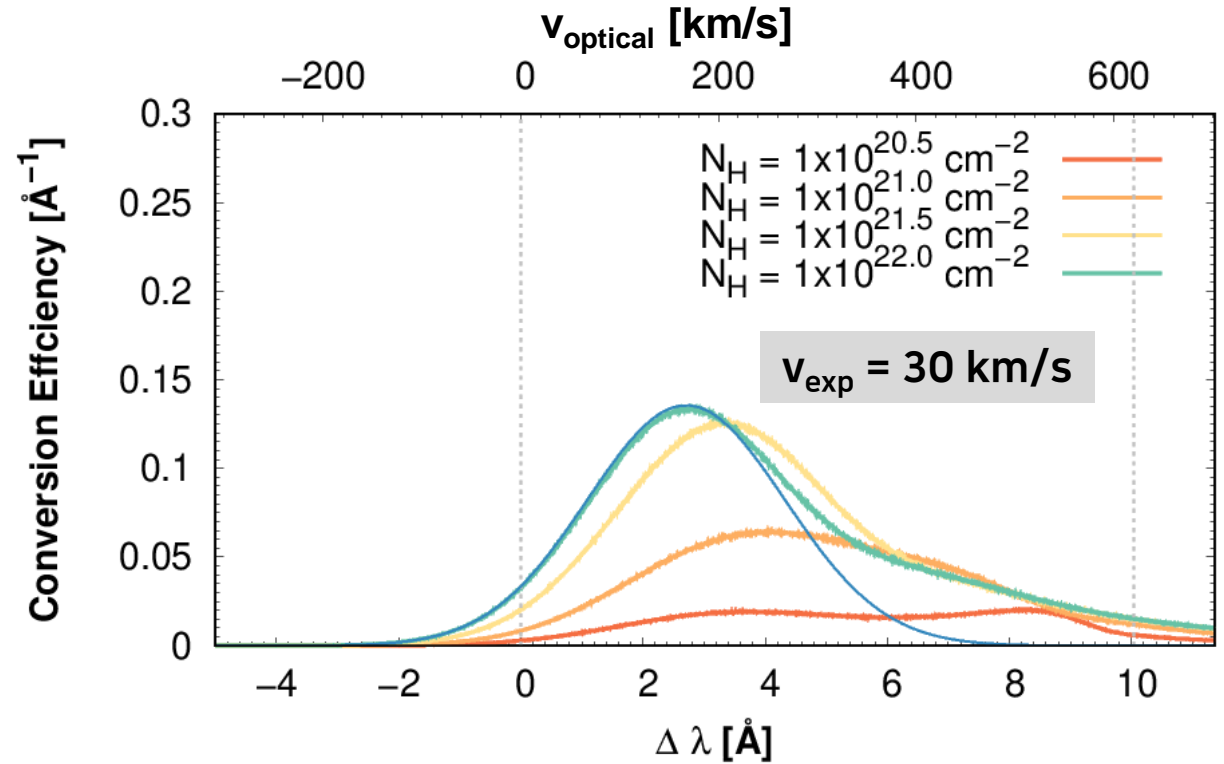


Result ② : Gaussian Source

- $v_{\text{cir}} = 20 \text{ km/s}$



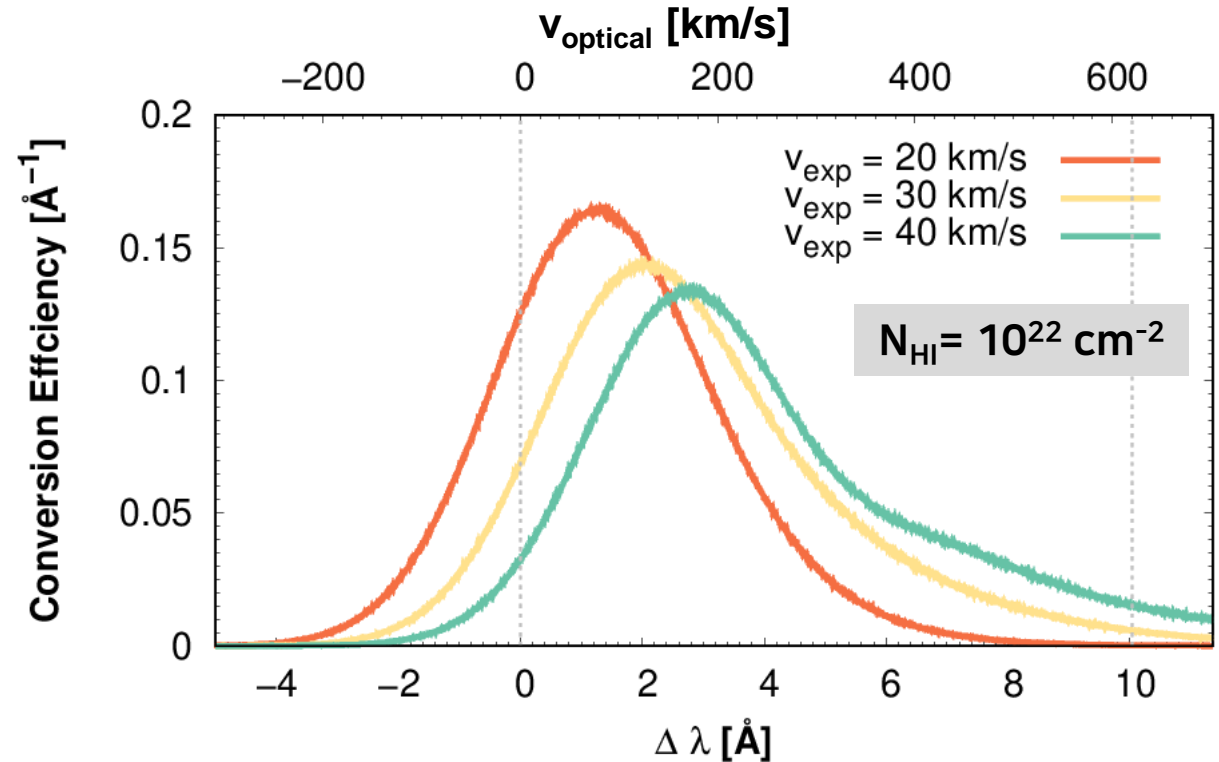
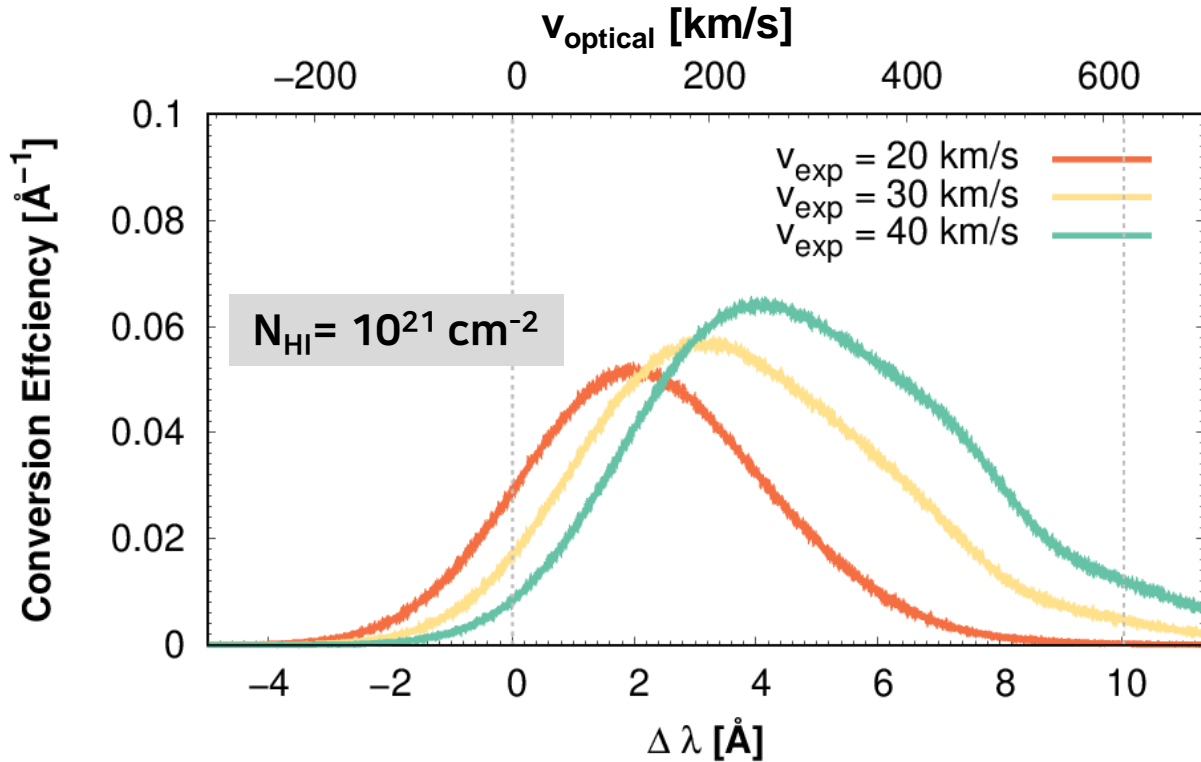
$v_{\text{Gaussian}} = 14.5 \text{ km/s}$



$v_{\text{Gaussian}} = 33.5 \text{ km/s}$

Result ② : Gaussian Source

- $v_{\text{cir}} = 20 \text{ km/s}$



Future Work

- We will conduct statistical analyses for profile distortion – line center, width and skewness
- We will extend our analysis to the case of open geometry, which will yield additional information including inclination.
- Profile fitting should be carried out using observational data with excellent signal to noise ratio allowing reliable continuum subtraction.